

# Air-quality modelling in the Lake Baikal region

Karen Van de Vel · Clemens Mensink · Koen De Ridder · Felix Deutsch ·  
Joachim Maes · Jo Vliegen · Artash Aloyan · Alexander Yermakov ·  
Vardan Arutyunyan · Tamara Khodzher · Bas Mijling

Received: 15 December 2008 / Accepted: 13 May 2009  
© Springer Science + Business Media B.V. 2009

**Abstract** In this paper, we assess the status of the air quality in the Lake Baikal region which is strongly influenced by the presence of anthropogenic pollution sources. We combined the local data, with global databases, remote sensing imagery and modelling tools. This approach allows to inventorise the air-polluting sources and to quantify the air-quality concentration levels in the Lake Baikal region to a reasonable level, despite the fact that local data are scarcely available. In the simulations, we focus on the month of July

2003, as for this period, validation data are available for a number of ground-based measurement stations within the Lake Baikal region.

**Keywords** Air quality · Lake Baikal · Pollution · Air pollution

## Introduction

Lake Baikal is the largest fresh water lake in the world, shaped as a half moon in a mountain hollow. The region around the lake is characterised by complex terrain, consisting of steep hill slopes covered with thick taiga and forests. In the mid-1990s, one of the major industrial zones of Siberia emerged along the Angara River located to the west of the lake. Today, there are several large cities and industrial centres such as Irkutsk, Angarsk, Cheremkovo and Usolye-Sibirskoye. The main industries are metal industry, energy, logging, oil and fuels, machine-building, chemicals, food industry and hydro-electricity. The total population of the metropolitan area amounts to over one million. Despite the fact that Lake Baikal houses the highest level of biodiversity in the world, it is under serious threat due to anthropogenic pollution. Besides water pollution, air pollution also forms a threat to the fauna and flora in and around the lake, as well as for the inhabitants of the Lake Baikal area. The Lake

---

K. Van de Vel (✉) · C. Mensink · K. De Ridder ·  
F. Deutsch · J. Maes · J. Vliegen  
Flemish Institute for Technological Research (VITO),  
Boeretang 200, 2400 Mol, Belgium  
e-mail: karen.vandavel@vito.be

A. Aloyan · V. Arutyunyan  
Russian Academy of Sciences,  
Institute for Numerical Mathematics,  
Moscow, Russia

A. Yermakov  
Russian Academy of Sciences, Institute of Energy  
Problems of Chemical Physics, Moscow, Russia

T. Khodzher  
Russian Academy of Sciences – Siberian Branch,  
Limnological Institute, Irkutsk, Russia

B. Mijling  
Royal Netherlands Meteorological Institute,  
De Bilt, The Netherlands

Baikal region is one of the areas in Siberia experiencing high level of air pollution (Cofala et al. 2005). However, local air quality data, both emission levels for pollutants as well as air quality concentrations measurements, are sparse.

We combined the available local data with global databases, remote sensing imagery and modelling tools in order to assess the air quality in the Lake Baikal region. The emission mapping (E-MAP) GIS tool was applied in order to set up an emission inventory. E-MAP combines local emission data (bottom-up approach) with the top-down emission methodology, in order to represent the actual situation as closely as possible. The regional-scale air quality model AURORA has been used in order to analyse the air quality situation and local air flow patterns. The AURORA model is driven by the advanced regional prediction system (ARPS) meteorological model and the E-MAP emission data. We determined the pollution levels for the month of July 2003.

The remainder of this paper is organised as follows. In “[Study domain and spatial data processing](#)”, a description is given of the study area together with the spatial data employed in order to characterise the study domain. “[Meteorological calculations](#)” describes the ARPS meteorological calculations that provide input for the AURORA air quality model. “[Emission modelling](#)” gives a description of the E-MAP methodology to calculate pollutant emissions. The meteorological fields and the emissions are subsequently used in the 3-D regional-scale air quality model AURORA which is presented in “[The AURORA air quality model](#)”. “[Meteorological and air quality simulations](#)” presents the validation results, and conclusions are drawn in “[Conclusions](#)”.

### Study domain and spatial data processing

The study area is located in Southeastern part of Siberia, Russia, as shown in Fig. 1; the domain is  $150 \times 150 \text{ km}^2$  at a resolution of 3 km. As mentioned in the “[Introduction](#)” it contains the major part of the Lake Baikal together with several large cities and industrial centres, including Irkutsk,

Angarsk, Chermkovo and Usolye-Sibirskoye, to the west of the lake.

In order to drive the atmospheric models (for meteorology (ARPS) and air quality (AURORA)) as well as the E-MAP emission model, we need to characterise the land surface. Below, we describe the different types of spatial data used.

The land use map (second panel of Fig. 1) was derived from the Global Land Cover (GLC2000) database of Joint Research Center (ref). The GLC2000 database is a global gridded 1-km resolution land cover map. It contains over 18 different land use categories. For the sake of the model requirements, these land use categories were aggregated to a smaller number of classes. As shown in Fig. 1, this yields the following categories: water bodies, continuous urban, discontinuous urban, industrial, pasture, crops, forest, snow/ice and shrubs.

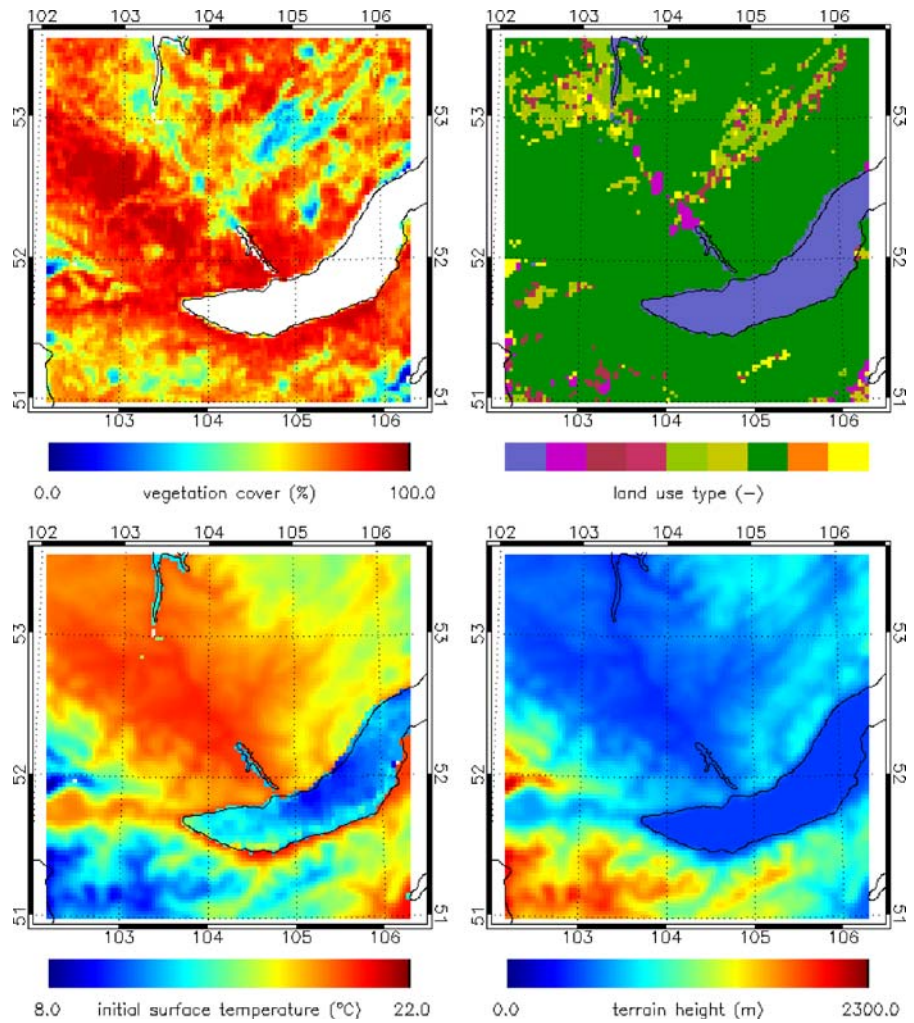
From Fig. 1, it can be seen that the built-up land use types are mainly located in the Angara valley. The major part of the study domain is covered by the natural-agricultural land use types.

For the meteorological and air quality modeling, one needs to specify the fractional green vegetation cover of each model grid cell at the surface. This value was derived from the normalized difference vegetation index (NDVI) taken from SPOT-VEGETATION imagery. The left panel in Fig. 1 shows a monthly mean fractional green vegetation cover for the month of July 2003, the inhabited areas (sparse vegetation) contrast to the more rural areas (vegetation more abundant).

The third panel in Fig. 1 shows the land and water surface temperatures for July 2003, with the warmer lake water temperature during summer time. The land surface temperature is a monthly average of the final analysis (FNL) meteorological data from the US National Centre for Environmental Prediction (NCEP). The water surface temperature has been derived from MODIS imagery.

Terrain height was interpolated from the Global 30 arcsec elevation dataset distributed by the US Geological Survey (right panel in Fig. 1). The southern part of the Lake Baikal is especially surrounded by steep hills.

**Fig. 1** Simulation domain for the atmospheric models, with centre at longitude 104.25° and latitude 52.3°, at 3 km resolution, covering 150 × 150 km<sup>2</sup>, including the lake Baikal and the city of Irkutsk. The *upper-left panel* gives the satellite-derived percentage vegetation cover. The *upper-right panel* shows the land use types, as follows: water (1), continuous urban (2), discontinuous urban (3), industrial (4), pasture (5), crops (6), forest (7), snow/ice (8), shrubs (9). The *lower-left panel* specifies the land and water surface temperature. The *lower-right panel* gives the terrain height



Other types of geographical information are required for the emission modelling, amongst others, the spatial distributions of population density (total, urban and rural) and the position of roads. The population density and road distribution was obtained from global databases. (LANDSCAN-ORNL, global gridded 1-km population density).

In order to account for pollution sources and air pollution outside the actual study domain, both the ARPS and AURORA models have nesting capabilities, such that these effects can enter the domain through the lateral boundaries. In this study, we used three nesting steps in order to go from a large domain at coarse resolution to the domain of interest at high resolution. The

outermost model domain was taken 1,800 km wide at 30-km resolution. The lateral boundary conditions used for this outer domain are mentioned in “[Meteorological calculations](#)” (meteorology) and “[The AURORA air quality model](#)” (air quality), respectively. Within this domain, a smaller domain was nested with a spatial extension of 500 km and a resolution of 10 km. Within the latter, a still smaller domain covering an area of 150 × 150 km<sup>2</sup> and a resolution of 3 km. This is the final domain as shown in Fig. 1, as it contains the Southern Lake Baikal together with the major cities in the area west of the lake.

Figure 2 gives an overview of the interplay between the different resolution simulations as well

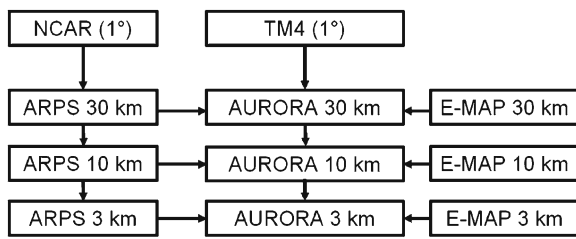


**Fig. 2** Schematic overview of the AURORA-ARPS-E-MAP coupling as well as the interplay between the different nesting levels

as of the interplay between the ARPS meteorological and AURORA air quality models; they are defined on exactly the same model domain. The E-MAP emission tool calculates air emissions at every resolution level within the nesting chain.

### Meteorological calculations

Meteorological fields, required for the AURORA model, were simulated using the ARPS, a non-hydrostatic mesoscale atmospheric model developed at the University of Oklahoma (Xue et al. 2000, 2001). The finite-difference equations of the model are discretised on an Arakawa C-grid, employing terrain-following coordinates. Advection is solved with a fourth order central-differencing scheme and leapfrog time stepping. Turbulence is represented by the 1.5 order turbulence model and the Sun and Chang (1986) parameterisation for the convective boundary layer. ARPS contains detailed parameterisations for cloud microphysics, cumulus convection and radiation transfer. As mentioned in “[Study domain and spatial data processing](#)”, ARPS has nesting capabilities, allowing large-scale atmospheric features to enter the domain through the lateral boundaries. In order to specify the lateral boundary conditions for the meteorological model (run at 30 km resolution), we make use of archived output data from the FNL data from the US NCEP as illustrated in Fig. 2. These data are provided at a six-hourly time step, and at a resolution of 1° (approx 100 km), they were interpolated to the model grid. A detailed land surface scheme (De Ridder and Schayes 1997) was incorporated in

ARPS to calculate the energy and water fluxes between the land surface and the atmosphere, including the effects of vegetation and soils on the partitioning of incident radiant energy between the turbulent fluxes of sensible and latent heat and the storage heat flux. In order to better represent urban surfaces, the land surface model was modified by including the Brutsaert (1975) temperature roughness parameterisation (De Ridder 2006).

### Emission modelling

The AURORA air quality model needs a correct specification of the position and the strength of the emission sources. AURORA distinguishes between ten anthropogenic emission classes and also takes biogenic emissions into account. In order to represent the actual situation as closely as possible, emission data from different sources were combined: local data supplemented with global or national emission inventories.

For the Irkutsk area, local emission data were obtained for the sectors of industry and for communal heating systems and for the pollutants  $\text{NO}_x$ ,  $\text{SO}_2$  and  $\text{CO}$ . We note that emissions related to building heating are of little importance for the simulation period (July 2003) as high temperatures were recorded (see “[Meteorological and air quality simulations](#)”).

For the areas within the three study domains where no local emission data were available, as well as for the other emission sectors, emission data were obtained with the E-MAP GIS tool (Maes et al. 2009). E-MAP performs a spatial disaggregation of the Emission Database for Global Atmospheric Research (EDGAR 3.2; Olivier and Berdowski 2001) emission inventory by using spatial surrogate data. The spatial variables include the data mentioned in “[Study domain and spatial data processing](#)”. The EDGAR 3.2 emission inventory uses the top-down approach (Samaras et al. 1995) in order to estimate emissions. Anthropogenic emissions of  $\text{NO}_x$ ,  $\text{SO}_2$ ,  $\text{CO}$ , and non-methane VOC are available for the sectors of power generation, industry, traffic and the domestic sector, as well as for biomass burning.

The annual emissions are distributed temporally according to monthly (January–December),



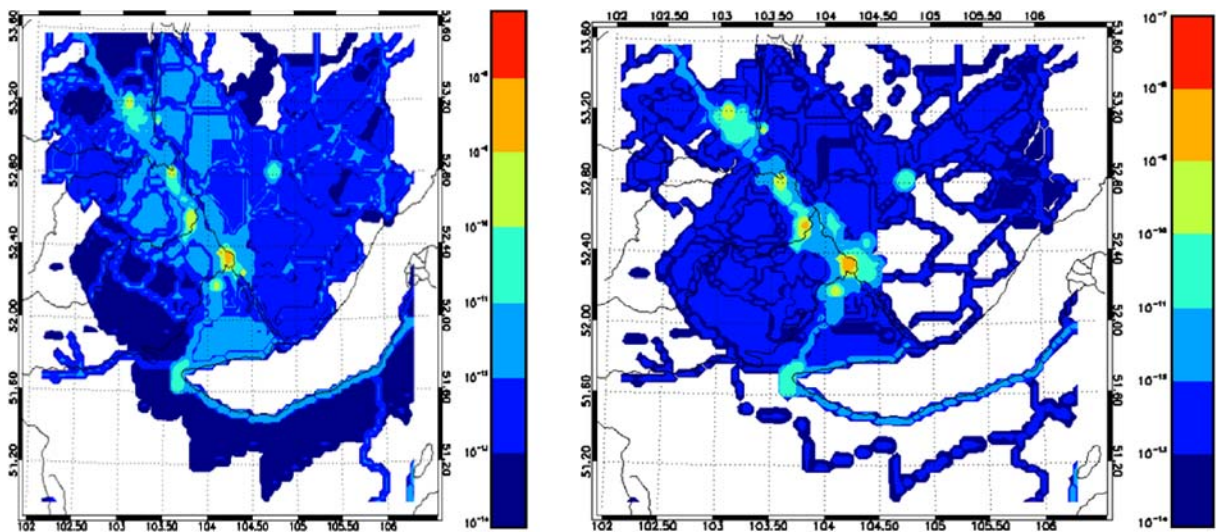


**Fig. 3** Emission maps for the 3-km resolution domain showing  $\text{NO}_2$  (left panel) and  $\text{SO}_2$  (right panel) emissions

daily (Monday–Sunday) and hourly (0–23 h) factors. These factors are specific to each pollutant and emission sector and, hence, reflect the different energy-use patterns as a function of time.

Apart from the above-mentioned emissions, biogenic emissions from forests were calculated following the methodology described in Simpson et al. (1999), using the land cover data mentioned previously as well as temperature and shortwave radiation values simulated by the ARPS meteorological model.

Figure 3 shows a 2-D plot of  $\text{NO}_x$  emissions (summed over all emission sectors) for the 3-km resolution domain. One can clearly distinguish the city of Irkutsk as well as the industrialised areas in the Angara valley.

### The AURORA air quality model

Regional-scale air quality was calculated with the atmospheric transport-chemistry model AURORA (‘Air quality modelling in urban regions using an optimal resolution approach’, see De Ridder et al. 2008).

In AURORA, advection is treated using the Walcek (2000) scheme, which is monotonic, exhibits a relatively limited numerical diffusion

and comes at a reasonable computational cost. Vertical diffusion is calculated with the Crank–Nicholson method (De Ridder and Mensink 2002). For dry deposition, AURORA uses the Wesely and Hicks (2000) formalism based on a resistance network. While the aerodynamic resistance and the laminar resistance can be readily calculated from the frictional velocity, the canopy resistance depends on the land use type as well as on the degree of vegetation in a grid cell.

The gaseous-phase chemistry is treated by means of the Carbon–Bond IV scheme (Gery et al. 1989), which was enhanced to include the effect of biogenic isoprene and terpene emissions. It covers the chemical reactions in the gas phase and accounts for the formation of oxidants in the atmosphere, e.g. ozone, sulphuric acid and nitric acid. Particulate matter concentrations were calculated although only for secondary aerosols as there are no emission data available for primary particulate matter. As we do not dispose of emission data for all pollutants and given the fact that no boundary conditions are available for particulate species (see below), we used empirical relations for the gas-to-particle conversion to sulfate, ammonium and nitrate aerosols (Van Egmond and Kesseboom 1985; Calvert et al. 1978; De Leeuw et al. 1990).

Large-scale pollutant concentrations, which are required to account for remote emission sources, were interpolated from output generated by the chemistry-transport model TM4 (van Noije et al. 2006) as shown in Fig. 2. TM4 is an offline 3-D model which provides concentration levels for gaseous species; TM4 is driven by assimilated meteorological fields from the European Centre for Medium-Range Weather Forecasts. It has a horizontal resolution of  $3 \times 2^\circ$  with 25 layers in the vertical. For the particulate species, zero-boundary conditions were applied for the outer domain.

### Meteorological and air quality simulations

The ARPS/AURORA simulations were performed for the month of July 2003. Only results from the smallest model domain will be presented, unless stated otherwise. In the next subsections, the validation of the individual model results for emissions, meteorology and air quality are discussed.

#### Emission validation

In order to assess the uncertainty involved in the emission estimates (which provide crucial input for the air quality modelling), it is of interest to compare the two datasets that are available: on one hand, the local emission data, and the top-down EDGAR 3.2 emission database on the other hand. As mentioned in “[Meteorological calculations](#)”, this comparison is only possible for the sectors of industry and communal heating for the pollutants of  $\text{NO}_x$ ,  $\text{SO}_2$  and CO.

Table 1 displays the totals from the Irkutsk bottom-up emission inventory and the EDGAR emission inventory (Russia total), for the sectors of industry and residential area, and this for the pollutants CO,  $\text{NO}_x$  and  $\text{SO}_2$ .

It can be seen that for CO, the industrial emission total for Irkutsk is higher than the total Russian emissions. The  $\text{NO}_x$  and  $\text{SO}_2$  industrial emission numbers for the Irkutsk area constitute 5.8%, 1.6%, respectively, of the national total. This indicates that there is a high uncertainty in-

**Table 1** Comparison between the bottom-up emission inventory for the Irkutsk area, and the EDGAR data for Russia

Emission [Gg]	CO	$\text{NO}_x$	$\text{SO}_2$
Irkutsk—industry	175.53	20.10	14.00
Irkutsk—residential	119.89	10.38	8.27
Russia (EDGAR-F10)	137.93	348.96	861.72
Russia (EDGAR-F40)	5436.99	412.09	981.70

Data are shown for the pollutants  $\text{NO}_2$ ,  $\text{SO}_2$  and CO, for the sector of industry (EDGAR F10) and the residential sector (EDGAR F40)

involved in the emission estimates, probably as well as in the local data and in the EDGAR data.

#### ARPS validation

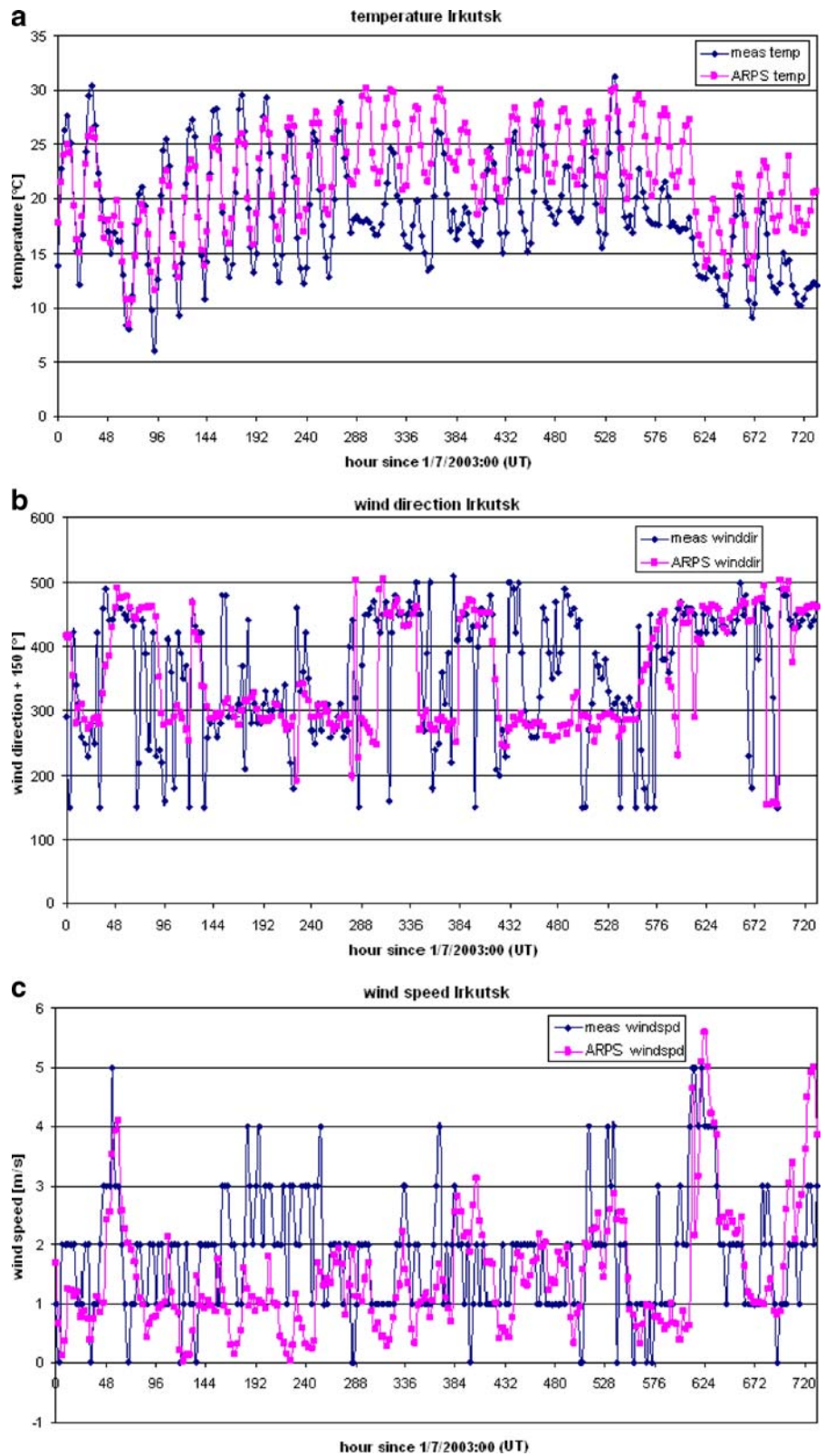
ARPS simulation results were validated by comparing model output with observed meteorological parameters, from a measurement station in the city of Irkutsk. Figure 4 shows validation results for surface air temperature, wind speed and wind direction for the period 1–31 July 2003. The simulated values are in fair agreement with the observations, and in particular, the temperature drop on the 27th of July is well captured.

We already mentioned that the Lake Baikal is a huge water body surrounded by steep mountains (especially the Southern part) as also can be seen from the right panel of Fig. 1. During daytime, often a strong uphill lake breeze is observed; this is a combined effect of (1) the land surface being hotter than the water surface and (2) the mountain slopes heating up more intensely than the valley areas. An example is shown in the right part of Fig. 5. At night, the situation reverses, producing a down-sloping land breeze, as exemplified in the left panel of Fig. 5.

#### AURORA validation

Figure 6 shows the monthly average (July 2003)  $\text{O}_3$  field for the 3-km resolution domain. The simulated formations of  $\text{O}_3$  plumes are mainly located in northwestern directions downwind of the urban and industrialised areas. Relatively low ozone concentrations are found in the densely populated and industrialised areas where the  $\text{NO}_x$  emissions are high as can be seen from Fig. 3. This indicates

**Fig. 4** Validation of simulated surface air temperature (*upper panel*), wind direction (*middle panel*) and wind speed (*lower panel*) at the station of Irkutsk, for the period the month of July 2003. The *solid lines* corresponding with the simulation result and the *symbols* with the observed values



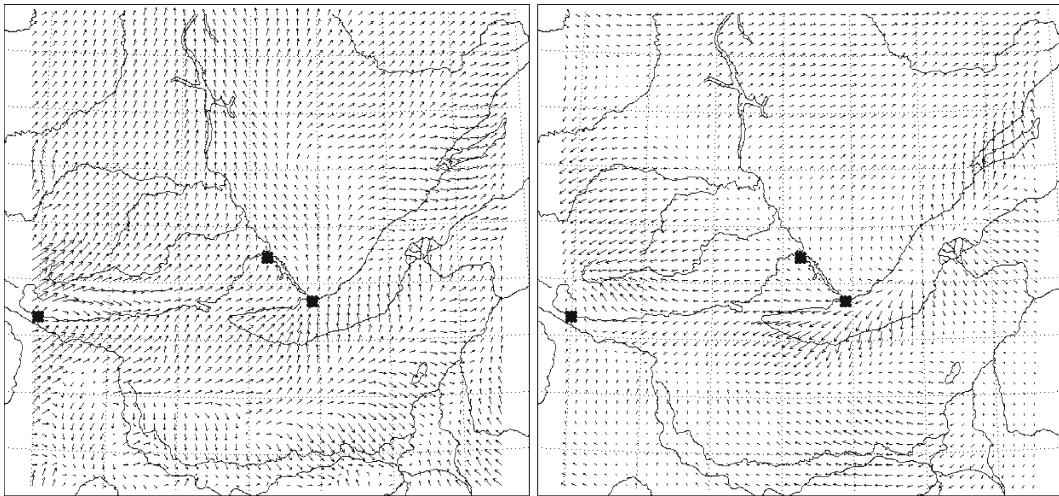


**Fig. 5** Two-dimensional wind fields showing the wind direction (*direction of arrows*) and wind speed (*length of arrows*), with the maximum length corresponding with a wind speed of 7 m/s). The area covered is the same as in Fig. 1, measurement stations are shown with stars: the

station of Listvyanka (close to Lake Baikal) is lying in the East, the station of Irkutsk in the North and the station of Mondy in the West. The *left panel* shows a night breeze on 2nd July 2003 at 4 A.M. local time, the *right panel* shows a day breeze on 3rd July 2003 at 3 P.M. local time

a VOC-limited regime over the urban areas. However, as discussed out below, it is possible that the  $\text{NO}_x$  emissions are too high for the Irkutsk urban area.

The concentration levels simulated with the AURORA model were compared to ground-based measurements obtained from three stations in the study area, at Irkutsk (lat.  $52.23^\circ$ , lon.

$104.25^\circ$ ), Listvyanka (lat.  $51.85^\circ$ , lon.  $104.9^\circ$ ) and Mondy (lat.  $51.67^\circ$ , lon.  $101.0^\circ$ ). The position of the measurement stations are indicated with stars in Fig. 5. The station of Irkutsk is located in an urban area with industrial activities, too; the Listvyanka station (close to the Lake Baikal) is a more rural site; the station of Mondy (most westerly station) can be considered as a rural background station. We note that the station of Mondy does not lie within the 3-km resolution domain; for this station, we, hence, use the 10-km resolution concentration fields to perform the comparison.

The monthly average  $\text{O}_3$  concentration for Mondy (derived from the 10-km resolution domain) amounts to  $86 \mu\text{g}/\text{m}^3$ ; this compares well with a measured  $\text{O}_3$  concentration of approximately  $80 \mu\text{g}/\text{m}^3$  (averaged over the years 1997–1999; Holloway et al. 2008).

All three stations measure concentrations for  $\text{HNO}_3$ ,  $\text{HCl}$ ,  $\text{NH}_3$ ,  $\text{SO}_2$  and for several ions. As we do not dispose of  $\text{NH}_3$  emissions, we will focus in the validation on the following species:  $\text{HNO}_3$ ,  $\text{SO}_2$ ,  $\text{SO}_4^{2-}$  and  $\text{NO}_3^-$ .

Before comparing the observed and modelled concentrations of air pollutants, a general remark has to be made: The fact that observed concen-

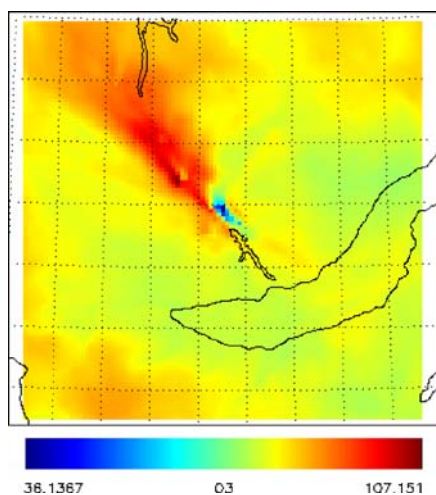


**Fig. 6** Monthly averaged  $\text{O}_3$  concentrations in  $\mu\text{g m}^{-3}$ , over the 3-km resolution domain



**Table 2** Simulated as compared to observed ground-level SO<sub>2</sub>, SO<sub>4</sub><sup>2-</sup>, HNO<sub>3</sub> and NO<sub>3</sub><sup>-</sup> concentrations for the stations of Irkutsk, Listvyanka and Mondy

	SO <sub>2</sub>	SO <sub>4</sub> <sup>2-</sup>	HNO <sub>3</sub>	NO <sub>3</sub> <sup>-</sup>	HNO <sub>3</sub> <sup>+</sup> NO <sub>3</sub> <sup>-</sup>
Irkutsk—model	5.89	2.19	1.58	1.79	3.37
Irkutsk—measurement	2.50	2.92	0.68	1.67	2.35
Listvyanka—model	1.84	1.74	0.19	1.31	1.50
Listvyanka—measurement	1.58	4.95	1.74	0.70	2.44
Mondy—model	1.26	1.04	0.04	0.85	0.89
Mondy—measurement	0.47	1.44	0.42	0.14	0.56

The simulated results are taken from the 3-km resolution AURORA calculations for the stations of Irkutsk and Listvyanka, whilst from the 10-km resolution calculations for the station of Mondy

trations of several “key pollutants” are unavailable, especially the ones of NO<sub>2</sub> (as precursor of HNO<sub>3</sub> and nitrates), O<sub>3</sub> (as most important photochemical pollutant governing all relevant oxidation processes) and NH<sub>3</sub> (as probably the main neutralizing agent of acids and important counterion of the nitrates and sulfates), makes a sound discussion of the results rather difficult.

Table 2 summarises the results for the pollutants HNO<sub>3</sub>, SO<sub>2</sub>, SO<sub>4</sub><sup>2-</sup> and NO<sub>3</sub><sup>-</sup>.

The overestimation of the SO<sub>2</sub> concentrations in Irkutsk is probably connected with an overestimation of the SO<sub>2</sub> emissions in the Irkutsk area. SO<sub>2</sub> concentrations in Listvyanka (with much less emission sources) are modelled well, in contrast. The (slight) overestimation of SO<sub>2</sub> in Mondy could be due to the lower resolution of the model domain at this location. We note that the same SO<sub>2</sub> concentration trends (high levels for Irkutsk and low levels for Listvyanka and Mondy) are observed for other summer months (Holloway et al. 2008; Hayami et al. 2008); in these studies, the modelled SO<sub>2</sub> concentration levels are of the same order of magnitude as the current results.

The conversion of SO<sub>2</sub> to sulphate is currently treated as a constant conversion rate in AURORA, derived from typically observed conversion rates in Northwestern Europe. Because this oxidation process does not proceed very fast, significant amounts of sulphate are usually found distant from the areas with strong sources. The modelled and measured SO<sub>4</sub> concentrations are in relatively good agreement for the three sites. Comparing the different sites, the measurements give a difference of a factor of 3, whilst the model results are different with a factor of 2.

The underestimation of HNO<sub>3</sub> and the overestimation of nitrate in Listvyanka and Mondy are connected due to an overestimation of the conversion of nitric acid to nitrate-aerosol in the model. Indeed the agreement between measurement and model is much better when summing up the two species. The HNO<sub>3</sub> concentration for Irkutsk is a factor of two too high probably due to an overestimation of the NO<sub>x</sub> emissions.

## Conclusions

A description was given of a numerical set up which combines spatial datasets and atmospheric models, aiming at an evaluation of the air quality in the Lake Baikal region for the month of July 2003.

In a first step, an overview was given of the geographical data processing needed in order to characterise the Lake Baikal region. These data were subsequently coupled to the E-MAP emission mapping GIS tool in order to generate detailed emissions for the study area. In a next step, the emission data and other spatial data were used as input into the transport-chemistry model AURORA. Together with meteorological fields simulated by the ARPS model, concentrations of pollutants were simulated.

In a validation exercise, it was shown that simulated temperature and wind speed showed a fair agreement with measured values. The ARPS meteorological model is also capable of simulating the lake breezes. The AURORA pollutant concentration levels compare relatively well with the available measurements. However, due to the lack

of a local data, it is difficult to obtain a complete air quality picture of the Lake Baikal region.

**Acknowledgements** The work described here was carried out with support of the Bilateral Scientific Cooperation Programme of the Flemish Government. The ARPS meteorological model was made available by the Center for Analysis and Prediction of Storms at the University of Oklahoma. We would also like to acknowledge the US Geological Survey for the GTOPO30 dataset, the Jet Propulsion Laboratory for the SST imagery, VITO for the SPOT-VEGETATION NDVI imagery and JRC for the Global Land Cover 2000 database.

## References

- Brutsaert, W. (1975). The roughness length for water vapour, sensible heat, and other scalars. *Journal of the Atmospheric Sciences*, *32*, 2028–2031. doi:10.1175/1520-0469(1975)032<2029:TRLFVW>2.0.CO;2.
- Calvert, J. G., Su, F., Bottenheim, J. W., & Strausz, O. P. (1978). Mechanism of the homogeneous oxidation of sulfur dioxide in the troposphere. *Atmospheric Environment*, *12*, 197–226.
- Cofala, J., Amann, M., & Mechler, R. (2005). *Scenarios of world anthropogenic emissions of air pollutants and methane up to 2030*. Report of the Transboundary Air Pollution (TAP) programme, International Institute for Applied Systems Analysis, Laxenburg, Austria.
- De Leeuw, F. A. A. M., Rheineck Leyssius, H. J., & Builtjes, P. J. H. (1990). Calculation of long term averaged ground level ozone concentrations. *Atmospheric Environment*, *24*(1), 185–193.
- De Ridder, K. (2006). Testing Brutsaert's temperature roughness parameterization for representing urban surfaces in atmospheric models. *Geophysical Research Letters*, *33*, L13403. doi:10.1029/2006GL026572.
- De Ridder, K., Lefebvre, F., Adriaensen, S., Arnold, U., Beckroge, W., Bronner, C., et al (2008). Simulating the impact of urban sprawl on air quality and population exposure in the German Ruhr area. Part II: Development and evaluation of an urban growth scenario. *Atmospheric Environment*, *42*, 7070–7077.
- De Ridder, K., & Mensink, C. (2002). Improved algorithms for advection and vertical diffusion in AURORA. In C. Borrego, & G. Schayes (Eds.), *Air pollution modeling and its application XV* (pp. 395–401). New York: Kluwer.
- De Ridder, K., & Schayes, G. (1997). The IAGL land surface model. *Journal of Applied Meteorology*, *36*, 167–182. doi:10.1175/1520-0450(1997)036<0167:TILSM>2.0.CO;2.
- Gery, M. W., Whitten, G. Z., Killius, J. P., & Dodge, M. C. (1989). A photochemical kinetics mechanism for urban and regional scale computer modeling. *Journal of Geophysical Research*, *94*, 925–956. doi:10.1029/JD094iD10p12925.
- Hayami, H., Sakurai, T., Han, Z., Ueda H., Carmichael, G. R., Streets, D., et al. (2008). MICS-Asia II: Model intercomparison and evaluation of particulate sulphate, nitrate and ammonium. *Atmospheric Environment*, *42*, 3510. doi:10.1016/j.atmosenv.2007.08.057.
- Holloway, T., Sakurai, T., Han, Z., Ehlers, S., Spak, S. N., Horowitz, L. W., et al. (2008). MICS-Asia II: Impact of global emissions on regional air quality in Asia. *Atmospheric Environment*, *42*, 3543. doi:10.1016/j.atmosenv.2007.10.022.
- Maes, J., Vliegen, J., Van de Vel, K., Janssen, S., Deutsch, F., De Ridder, K., et al. (2009). Spatial surrogates for the disaggregation of CORINAIR emission inventories. *Atmospheric Environment*, *43*(6), 1246–1254.
- Olivier, J. G. J., & Berdowski, J. J. M. (2001). In J. J. M. Berdowski, R. Guicherit, & B. J. Heij (Eds.), *Global emissions sources and sinks, the climate system* (pp. 33–78). Lisse: Balkema.
- Samaras, Z., Kyriakis, N., & Zachariadis T. (1995). Reconciliation of macroscale and microscale motor vehicle emission estimates. *Science of the Total Environment*, *169*, 231–239.
- Simpson, D., Winiwarter, W., Borjesson, G., Cinderby, S., Ferreira, A., Guenther, A., et al. (1999). Inventorying emissions from nature in Europe. *Journal of Geophysical Research*, *104*, 8113–8152. doi:10.1029/98JD02747.
- Sun, W. Y., & Chang, C. Z. (1986). Diffusion model for a convective layer. Part I: Numerical simulation of convective layer. *Journal of Climate and Applied Meteorology*, *25*, 1445–1453. doi:10.1175/1520-0450(1986)025<1445:DMFACL>2.0.CO;2.
- Van Egmond, N. D., & Kesseboom, H. (1985). A numerical mesoscale model for long-term average NOx and NO2-concentration. *Atmospheric Environment*, *19*, 587–595.
- van Noije, T. P. C., Eskes, H. J., Dentener, F. J., Stevenson, D. S., Ellingsen, K., Schultz, M. G., et al. (2006). Multi-model ensemble simulations of tropospheric NO2 compared with GOME retrievals for the year 2000. *Atmospheric Chemistry and Physics Discussion*, *6*, 2965–3047.
- Walcek, C. J. (2000). Minor flux adjustment near mixing ratio extremes for simplified yet highly accurate monotonic calculation of tracer advection. *Journal of Geophysical Research*, *105*, 9335–9348. doi:10.1029/1999JD901142.
- Wesely, M. L. & Hicks, B. B. (2000). A review of the current status of knowledge on dry deposition. *Atmospheric Environment*, *34*, 2261–2282.
- Xue, M., Droegemeier, K. K., & Wong, V. (2000). The Advanced Regional Prediction System (ARPS)—a multiscale nonhydrostatic atmospheric simulation and prediction tool. Part I: Model dynamics and verification. *Meteorology and Atmospheric Physics*, *75*, 161–193. doi:10.1007/s007030070003.
- Xue, M., Droegemeier, K. K., Wong, V., Shapiro, A., Brewster, K., Carr, F., et al. (2001). The Advanced Regional Prediction System (ARPS)—a multiscale nonhydrostatic atmospheric simulation and prediction tool. Part II: Model physics and applications. *Meteorology and Atmospheric Physics*, *76*, 134–165. doi:10.1007/s007030170027.